

Spatio-temporal variability of biophysical parameters of irrigated maize using orbital remote sensing

Variabilidade espaço-temporal de parâmetros biofísicos do milho irrigado utilizando sensoriamento remoto orbital

Taiara Souza Costa^{1*}; Robson Argolo dos Santos²; Rosângela Leal Santos³; Roberto Filgueiras⁴; Fernando França da Cunha⁵; Anderson de Jesus Pereira⁶; Rodrigo Amaro de Salles⁷

Highlights

Use of orbital remote sensing in irrigation management.
Estimation of dry biomass as a possibility of predicting final yield.
Spatio-temporal dynamics of actual crop evapotranspiration.

Abstract

This study proposes to estimate the actual crop evapotranspiration, using the SAFER model, as well as calculate the crop coefficient (K_c) as a function of the normalized difference vegetation index (NDVI) and determine the biomass of an irrigated maize crop using images from the Operational Land Imager (OLI) and Thermal Infrared (TIRS) sensors of the Landsat-8 satellite. Pivots 21 to 26 of a commercial farm located in the municipalities of Bom Jesus da Lapa and Serra do Ramalho, west of Bahia State, Brazil, were selected. Sowing dates for each pivot were arranged as North and South or East and West, with cultivation starting firstly in one of the orientations and subsequently in the other. The relationship between NDVI and the K_c values obtained in the FAO-56 report ($K_{c,FAO}$) revealed a high coefficient of determination ($R^2 = 0.7921$), showing that the variance of $K_{c,FAO}$ can be explained by NDVI in the maize crop. Considering the center pivots

¹ Student of the Master's Course of the Graduate Program in Agricultural Engineering, Universidade Federal de Viçosa, UFV, Viçosa, MG, Brazil. E-mail: taiarasouzacosta1@gmail.com

² Student of the Doctoral Course of the Graduate Program in Agricultural Engineering, UFV, Viçosa, MG, Brazil. E-mail: argolo.agro@gmail.com

³ Profa Dra, Technology Department, Universidade Estadual de Feira de Santana, UEFS, BA, Brazil. E-mail: rosangela.leal@gmail.com

⁴ Dr., Department of Agronomic Engineering, UFV, Viçosa, MG, Brazil. E-mail: betofilgueiras@gmail.com

⁵ Prof., Department of Agronomic Engineering, UFV, Viçosa, MG, Brazil. E-mail: fernando.cunha@ufv.br

⁶ Student of the Master's Course of the Irrigation and Drainage, Universidade Estadual Paulista, UNESP, São Paulo, SP, Brazil. E-mail: agroandersonn@gmail.com

⁷ Student of the Doctoral Course of the Phytotechnics, UFV, Viçosa, MG, Brazil. E-mail: rodrigoamarodesalles@gmail.com

* Author for correspondence

with different planting dates, the crop evapotranspiration (ET_c) pixel values ranged from 0.0 to 6.0 mm d⁻¹ during the phenological cycle. The highest values were found at 199 days of the year (DOY), corresponding to around 100 days after sowing (DAS). The lowest BIO values occur at 135 DOY, at around 20 DAS. There is a relationship between ET_c and BIO, where the DOY with the highest BIO are equivalent to the days with the highest ET_c values. In addition to this relationship, BIO is strongly influenced by soil water availability.

Key words: Agrometeorological models. Irrigation management. Phenological cycle.

Resumo

Objetivou-se com o presente estudo estimar a evapotranspiração real da cultura por meio do modelo SAFER, calcular o K_c em função do NDVI e a biomassa da cultura do milho irrigado, utilizando para isso imagens dos sensores *Operacional Land Imager* (OLI) e *Thermal Infrared Sensor* (TIRS) do satélite Landsat-8. Foram selecionados os pivôs 21 ao 26 de uma fazenda comercial localizada nos municípios de Bom Jesus da Lapa e Serra do Ramalho, situadas no oeste do estado da Bahia, Brasil. As épocas de semeadura dentro dos pivôs são ordenadas em Norte e Sul ou Leste e Oeste, iniciando o cultivo primeiro em uma das orientações e posteriormente na outra. Verifica-se com base na relação entre NDVI e $K_{c_{FAO}}$, um alto valor do coeficiente de determinação ($R^2=0,7921$), evidenciando que a variância do $K_{c_{FAO}}$ pode ser explicada pelo NDVI na cultura do milho. Considerando-se os pivôs centrais com diferentes datas de plantio, os valores dos pixels da ET_c variaram de 0,0 a 6,0 mm d⁻¹ durante o ciclo fenológico. Os maiores valores foram encontrados para o DOY 199, correspondendo ao DAS em torno de 100 dias. Os valores mais baixos da BIO ocorrem aos 135 DOY em torno de 20 DAS. É observado que existe uma relação entre a ET_c e BIO, os DOY mais elevados da BIO são equivalentes com os maiores valores de ET_c . Além desta relação, a BIO é fortemente influenciada pela disponibilidade hídrica no solo.

Palavras-chave: Ciclo fenológico. Manejo da irrigação. Modelos agrometeorológicos.

Introduction

Irrigation management consists of the application of water at the right time and in the necessary amount for the crop (Bernardo, Mantovani, Silva, & Soares, 2019). Among the existing irrigation management methods, the weather-based approach is the most commonly used due to its easy execution and greater technical and economic viability (Althoff, Santos, Bazame, Cunha, & Filgueiras, 2019; Santos, Venancio, Filgueiras, & Cunha, 2020). In view of the importance of the crop coefficient (K_c) for weather-based irrigation management, various studies have examined

the modeling of this parameter as a function of the vegetation index and shown good results (Alface, Pereira, Filgueiras, & Cunha, 2019), as it is estimated using real field conditions.

It is worth stressing, however, that weather-based management considers the irrigation amount to be applied equally across the cultivated area (Martins, Busato, Silva, Rodrigues, & Reis, 2013). Therefore, studies that estimate the spatial and temporal variability of the actual crop evapotranspiration (ET_c) are relevant and provide basis for applying irrigation at a variable rate, replacing the adequate amount of water.

Agrometeorological models were thus developed for the spatial and temporal determination of ET_c via orbital remote sensing techniques. A noteworthy example of such methods is the Simple Algorithm for Evapotranspiration Retrieving (SAFER), presented by Teixeira (2010). The technique consists of an easy-to-apply algorithm (Teixeira, 2010) with good results demonstrated in studies focusing on irrigation management. In addition to the water demand, it also allows us to determine the daily increase in crop biomass (BIO). Knowing the BIO increase is important to predict the final yield of the crop, as done by Bastiaanssen and Ali (2003).

The above descriptions evidence the importance of knowing the spatio-temporal variability of crop parameters such as ET_c , K_c and the accumulated biomass increase in irrigated crops. On this basis, the present study was developed to estimate the ET_c using the SAFER model as well as calculate the K_c as a function of NDVI and the biomass of an irrigated maize crop using images from the Operational Land Imager (OLI) and Thermal Infrared (TIRS) sensors of the Landsat-8 satellite.

Material and Methods

The study site comprises center pivots of a commercial farm located in the municipalities of Bom Jesus da Lapa and Serra do Ramalho, west of Bahia State, Brazil. The municipality of Bom Jesus da Lapa is located by the coordinate pairs, with X1: -42.90936; Y1: -12.68917 as the upper-left corner and X2: -43.70607; Y2: -13.87617 as the lower-right corner. The municipality of Serra do Ramalho is also delimited by the coordinate pairs, with X1: -43.43047; Y1: -13.18179 as the upper-left corner and X2: -43.93314; Y2: -13.80629 as the lower-right corner. Both municipalities adopt the WGS84 coordinate reference system.

The farm performs crop rotation under 30 center pivots. In this study, we worked with the maize crop (Figure 1). Considering the most consistent data and orbital images free of the presence of clouds, pivots 21 to 26 were selected, totaling six pivots. Pivots 21 to 25 have an area of 45 ha each and pivot 26 has an area of 33 ha. Sowing dates for each pivots are arranged as North and South or East and West, with cultivation starting firstly in one of the orientations (bands of the center pivots) and subsequently in the other (Table 1).

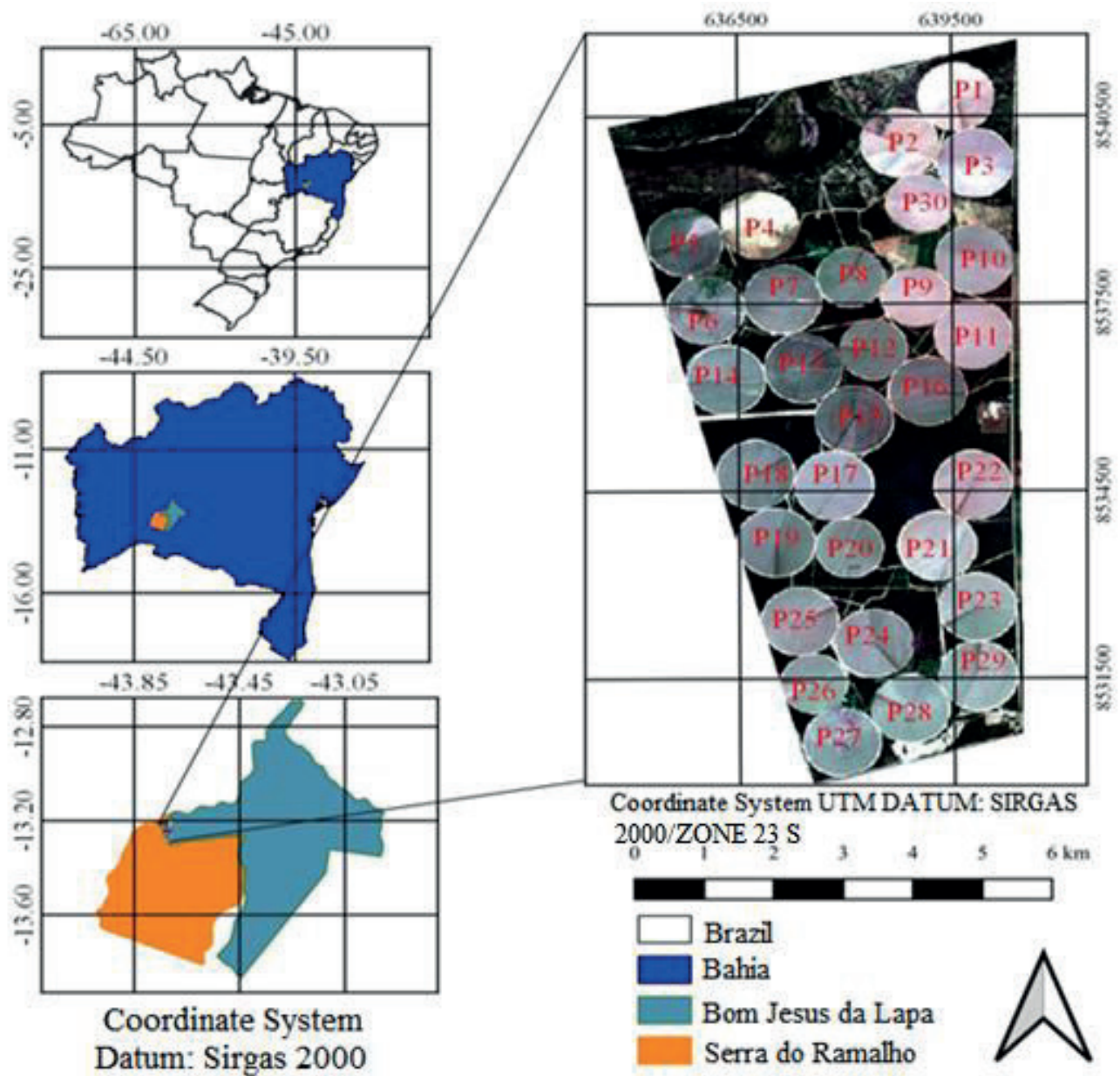


Figure 1. Geographic location of the study area indicating the municipalities covered, the state of Bahia and Brazil.

To estimate the biophysical parameters of the area, eight images from the year 2014 (04/13/2014, 05/15/2014, 05/31/2014, 07/02/2014, 07/18/2014, 08/19/2014, 09/04/2014 and 09/20/2014) were acquired from the OLI and TIRS sensors of the Landsat-8 satellite, with resolution of 30 and 100 m, respectively, and Level-1 processing. These images were acquired on the Earth Explorer platform, available at <http://earthexplorer.usgs.gov/> (United States Geological Survey [USGS], 2015). After the images were obtained, the

pre-processing procedures were performed in QGIS® 3.16 software (QGIS Development Team [QGIS], 2015) for converting digital numbers to physical values and atmospheric correction. Atmospheric correction was achieved using the DOS 1 (Dark Object Subtraction) method and the Semi-Automatic Classification plugin (Congedo, 2016). Subsequently, the SAFER algorithm was run, in which the biophysical parameters that compose the ETc were calculated.

Table 1
Information regarding the cultivation of irrigated maize

Pivot	PO	Area ha	Cv	Planting	EI	IA mm
21	Norte	45	1	04/24/2014	08/18/2014	392.48
21	Sul	45	1	04/23/2014	08/18/2014	371.65
22	Norte	45	1	04/26/2014	09/18/2014	520.15
22	Sul	45	1	04/25/2014	08/21/2014	507.11
23	Norte	45	1	04/17/2014	08/11/2014	358.67
23	Sul	45	1	04/28/2014	08/09/2014	378.76
24	Oeste	45	1	04/16/2014	08/09/2014	526.12
24	Leste	45	1	04/09/2014	08/10/2014	547.21
25	Norte	45	2	04/04/2014	07/28/2014	434.41
25	Sul	45	1	04/03/2014	07/28/2014	453.01
26	Norte	33	1	04/05/2014	08/04/2014	460.48
26	Sul	33	1	04/04/2014	08/02/2014	439.82

PO - Planting orientation; Cv - Cultivar; EI - End of irrigation; IA - irrigation amount applied in the cycle. 1- Dekalb 390 VT Pro 2 maize; 2- Dekalb 390 Conventional maize.

Actual crop evapotranspiration (ET_c)

To determine the ET_c from the SAFER algorithm, it is necessary to calculate the biophysical parameters displayed below. The first biophysical parameter estimated in SAFER was the albedo at the top of the

$$\alpha_{TOA} = 0.300\rho_2 + 0.277\rho_3 + 0.233\rho_4 + 0.143\rho_5 + 0.036\rho_6 + 0.012\rho_7 \quad (1)$$

where $\rho_2, \rho_3, \rho_4, \rho_5, \rho_6$ and ρ_7 are the surface reflectances of bands 2, 3, 4, 5, 6 and 7 (Equation 1); and $\alpha - 0.7$ and $b - 0.06$ (Equation 2) are the regression coefficients (Vanhellemont & Ruddick, 2014).

Surface temperature (T_s) was obtained using Equation 3. To calculate T_{bri} , band 10 (thermal) was used.

$$T_s = 1.11 \times T_{bri} - 31.89 \quad (3)$$

where ρ_{10} is the thermal infrared band of the TIRS sensor of Landsat 8 satellite.

The normalized difference vegetation index (NDVI) is an indicator related to the status of the plant from the red and near-infrared reflectance. Higher NDVI values translate into larger amounts of chlorophyll and, consequently, a greater productive potential of the plant (Rissini, Kawakami, & Genú, 2015). This index was calculated using Equation 4 (Rouse, Haas, Schell, & Deering, 1974).

$$NDVI = \frac{\rho_{nir} - \rho_r}{\rho_{nir} + \rho_r} \quad (4)$$

where ρ_{nir} is the reflectance in the near-infrared band (band 5); and ρ_r is the reflectance in the red band (band 4).

The evapotranspiration fraction (ET_f) (Equation 5) was determined using the α_s, T_s and NDVI biophysical parameters data.

atmosphere (α_{TOA}) (Equation 1), which makes it possible to estimate the other parameters (Equations 2, 3, 4, 5 and 6) and subsequently ET_c. From the α_{TOA} , the surface albedo (α_s) was calculated using Equation 2. The weights adopted to determine α_{TOA} were defined by the methodology of B. B. Silva et al. (2016).

$$\alpha_s = \alpha \times \alpha_{TOA} + b \quad (2)$$

$$ET_f = \exp \left[a + b \left(\frac{T_s}{\alpha_s \times NDVI} \right) \right] \quad (5)$$

where a and b are the regression coefficients obtained by the model of Teixeira (2010), which showed the respective values of 1.8 and -0.008, adjusted for the semi-arid conditions of Brazil.

Subsequently, the reference evapotranspiration (ET_o) in mm d⁻¹ was estimated by the FAO 56 Penman-Monteith method (Allen, Pereira, Raes, & Smith, 1998), using daily weather data from the weather station located at the study site (Equation 6).

$$ET_o = \frac{0.408 \Delta (R_N - G) + \gamma \left(\frac{900}{T + 273} \right) U_2 (e_s - e_a)}{\Delta + \gamma (1 + 0.34 \times U_2)} \quad (6)$$

where ET_o is the reference evapotranspiration (mm d⁻¹); Δ is the slope of the vapor pressure curve (kPa °C⁻¹); R_N is the net radiation at the crop surface (MJ m⁻² d⁻¹); G is the soil heat-flux density (MJ m⁻² d⁻¹); γ is the psychrometric constant (kPa °C⁻¹); T is the mean daily air temperature (°C); U_2 is the wind speed (daily mean) at a height of 2 m; e_s is the saturation vapor pressure (kPa); and e_a is the actual vapor pressure (kPa).

From the ET_o and ET_f data, ET_c was estimated in mm d⁻¹ using Equation 7.

$$ET_c = ET_f \times ET_o \quad (7)$$

Accumulated biomass (BIO)

Knowing the BIO is fundamental to make rational use of plants and to monitor nutrient cycling. In addition to allowing the calculation of grain yield, this variable is important for planning the logistics, storage and marketing of the crop even before the harvest (Higuchi, Santos, Ribeiro, Minette, & Biot, 1998). To determine the daily BIO increase, it was first necessary to determine the absorbed photosynthetically active radiation (APAR) by the crop (Bastiaanssen & Ali, 2003) (Equation 8).

$$APAR = (1.26 \times NDVI - 0.16) \times (0.48 \times R_G) \quad (8)$$

where R_G is the daily solar radiation ($W m^{-2}$); and NDVI is the normalized difference vegetation index.

Biomass production per unit area over time was calculated using the radiation model developed by Monteith (1972), according to Equation 9. The BIO variable represents how much biomass the plant added to its structure per day, in kilograms.

$$BIO = \epsilon_{max} \times ET_f \times APAR \times 0.864 \quad (9)$$

where BIO is the total biomass accumulated in the day ($kg ha^{-1} d^{-1}$; dry matter); ϵ_{max} is the maximum radiation use efficiency, which is $2.7 g MJ^{-1}$ for the maize crop (Bastiaanssen & Ali, 2003); 0.864 is the conversion factor that makes it possible to obtain biomass in $kg ha^{-1}$ (Teixeira, Scherer-Warren, Hernandez, Andrade & Leivas, 2013); and APAR is the absorbed photosynthetically active radiation.

Crop coefficient (Kc)

From the Kc values obtained in the FAO-56 report, here called Kc_{FAO} , and the NDVI values for each date of the images under study, expressed as a function of the crop cycle, a simple linear regression model (Equation 10) was fitted to estimate Kc by the NDVI, termed Kc_{NDVI} .

$$y = a_0 + b_i x_i \quad (10)$$

where y is the dependent variable, Kc_{FAO} ; x_i is the independent variable, $NDVI_{mean}$; and a_0 and b_i are the adjusted regression coefficients of the linear model.

Subsequently, the Kc_{NDVI} (Equation 10) was calculated for each day of the year (DOY) in the different bands of the center pivots. It is important to mention that this approach was chosen because different sowing dates were adopted for the different orientations of the center pivots.

For a better understanding of the results, as well as the descriptive statistics, graphs were developed using R software (R Core Team [R], 2016).

Results and Discussion

Table 2 shows the values of the meteorological variables measured on the dates the Landsat8 satellite images were acquired. During the phenological cycle, relative humidity (RH) showed an amplitude of 35.6%. The highest RH (67.2%) was observed at 103 DOY, which coincided with the beginning of the phenological cycle for center pivots P25 and P26, whose plants were sown on April 4th and 5th, 2014, in the North position and April 3 and 4, 2014, in the South position, respectively. For the other center pivots, however, the maize had not yet been sown.

Table 2
Climatic variables on the days of acquisition of the Landsat-8 images

DOY	Tmax °C	Tmin °C	RH %	U ₂ m s ⁻¹	RG W m ⁻²	ET _o mm d ⁻¹
103	34.1	19.8	67.2	0.5	262	4.60
135	33.6	17.9	51.5	0.5	230	4.04
151	32.4	19.7	51.0	1.0	213	4.18
183	35.7	19.7	40.4	0.7	215	4.14
199	32.8	17.9	45.5	0.6	206	3.75
231	31.1	17.2	38.7	1.7	255	5.86
247	37.4	18.9	31.6	0.8	260	6.10
263	39.5	22.9	32.1	1.1	282	7.62
Amplitude	8.4	5.7	35.6	1.2	69	3.87

DOY: day of the year; Tmax: maximum temperature; Tmin: minimum temperature; RH: relative humidity; U₂: wind speed at 2 m of height; R_G: incident solar radiation; ET_o: reference evapotranspiration.

The highest values of maximum and minimum temperature, ETo and RG were recorded at 263 DOY, which refers to the senescence period of the crop for pivots P21, P22, P23 and P24; and exposed soil for the other center pivots, as the maize had already been harvested. On that date, because it was the senescence period, there was no irrigation in the area. Reference evapotranspiration was highest because the meteorological variables were decisive for its estimate, with incident solar radiation (282 W m⁻²) being the parameter of greatest influence (Pandey, Dabral, & Pandey, 2016). The highest RH and the lowest U₂ occurred at 103 and 135 DOY. At 103 DOY, sowing had been only carried out under pivots 25 and 26, whose plants were at around nine days after sowing (DAS), whereas at 135 DOY the plants were at approximately 45 DAS for P23 North and P24. For the other pivots, the plants were at 25 DAS.

Table 3 shows the biophysical parameters throughout the irrigated maize cultivation cycle, for the different center pivots. The variables of α_s , NDVI and T_s are results of the status of the agroecosystems and allow the management of the crop to be directed to the more critical regions, generating significant gains to the production system (Ribeiro et al., 2017; Teixeira & Leivas, 2017). The highest mean α_s (0.19 to 0.25) and T_s (35.15 to 39.65 °C) occurred before sowing and after 168 DAS. These high values are due to the presence of exposed soil and the senescence of the crops; thus, evapotranspiration is reduced and the sensitive heat is greater at the expense of the reduction in latent heat of vaporization.

Table 3

Mean daily values and standard deviation of surface albedo (α_s), NDVI and surface temperature (T_s) on the different days after sowing (DAS) in irrigated maize

DAS	α_s	NDVI	T_s	DAS	α_s	NDVI	T_s
Center Pivot 21 - North				Center Pivot 21 - South			
BS*	0.19±0.0020	0.31±0.0070	33.75±0.50	BS*	0.18±0.0015	0.31±0.0101	32.75±0.55
21	0.14±0.0053	0.50±0.0161	28.85±1.26	22	0.14±0.0021	0.52±0.0162	27.85±0.81
37	0.12±0.0005	0.79±0.0053	21.25±0.16	38	0.12±0.0038	0.71±0.0102	20.95±0.30
69	0.12±0.0009	0.92±0.0032	24.15±0.22	80	0.12±0.0019	0.92±0.0075	24.25±0.41
85	0.13±0.0009	0.90±0.0023	20.95±0.21	86	0.13±0.0019	0.90±0.0085	20.75±0.28
111	0.13±0.0011	0.85±0.0075	24.85±0.25	112	0.13±0.0027	0.85±0.0172	24.75±0.42
127	0.13±0.0021	0.61±0.0293	30.35±0.19	128	0.14±0.0040	0.63±0.0572	29.15±0.40
143	0.17±0.0022	0.38±0.0044	34.25±0.22	144	0.16±0.0030	0.38±0.0141	34.05±0.29
Center Pivot 22 - North				Center Pivot 22 - South			
BS*	0.19±0.0020	0.32±0.0131	34.15±0.59	BS*	0.19±0.0020	0.33±0.0171	33.75±0.54
19	0.15±0.0017	0.45±0.0152	28.75±0.67	20	0.14±0.0050	0.48±0.0202	30.75±2.15
35	0.13±0.0010	0.61±0.0104	21.65±0.43	36	0.12±0.0008	0.59±0.0052	21.05±0.30
67	0.12±0.0007	0.91±0.0032	24.35±0.51	68	0.12±0.0007	0.92±0.0021	24.25±0.41
83	0.13±0.0010	0.90±0.0031	21.25±0.35	84	0.12±0.0009	0.90±0.0035	21.05±0.29
115	0.14±0.0011	0.85±0.0073	24.95±0.59	116	0.13±0.0011	0.86±0.0041	25.05±0.45
131	0.15±0.0022	0.51±0.0401	30.45±0.36	132	0.15±0.0018	0.66±0.0311	30.35±0.28
147	0.16±0.0020	0.38±0.0081	34.65±0.32	148	0.15±0.0019	0.38±0.0032	30.05±0.23
Center Pivot 23 - North				Center Pivot 23 - South			
BS*	0.18±0.0042	0.31±0.0123	33.85±0.58	BS*	0.19±0.0044	0.33±0.0243	33.55±0.43
28	0.13±0.0021	0.54±0.0412	26.45±0.45	22	0.13±0.0026	0.49±0.0212	27.45±0.43
44	0.12±0.0012	0.87±0.0072	20.85±0.26	38	0.12±0.0007	0.80±0.0051	21.05±0.23
76	0.12±0.0010	0.92±0.0041	24.35±0.43	70	0.12±0.0010	0.92±0.0024	24.35±0.34
92	0.13±0.0012	0.89±0.0034	24.85±0.33	86	0.13±0.0011	0.89±0.0024	20.55±0.29
124	0.15±0.0023	0.79±0.0401	26.25±0.51	118	0.15±0.0045	0.76±0.0691	26.65±0.73
140	0.15±0.0044	0.49±0.0244	31.45±0.35	134	0.15±0.0055	0.49±0.0483	31.55±0.45
156	0.16±0.0061	0.35±0.0082	35.55±0.31	150	0.17±0.0045	0.34±0.0091	35.45±0.30
Center Pivot 24 - West				Center Pivot 24 - East			
BS*	0.18±0.0035	0.15±0.0031	34.05±0.45	BS*	0.18±0.0022	0.16±0.0022	34.05±0.51
29	0.12±0.0011	0.53±0.0123	24.65±0.30	31	0.12±0.0014	0.38±0.0203	24.45±0.21
45	0.12±0.0010	0.68±0.0054	20.25±0.18	47	0.12±0.0009	0.58±0.0043	20.45±0.21
77	0.12±0.0010	0.92±0.0032	24.25±0.25	79	0.12±0.0008	0.92±0.0021	24.05±0.28
93	0.13±0.0020	0.89±0.0042	21.05±0.25	95	0.12±0.0013	0.89±0.0025	20.85±0.18
125	0.14±0.0036	0.78±0.0671	27.45±0.51	127	0.14±0.0022	0.76±0.0521	26.45±0.32
141	0.15±0.0041	0.40±0.0201	31.45±0.18	143	0.16±0.0021	0.46±0.0182	31.15±0.20
157	0.17±0.0078	0.34±0.0135	35.05±0.26	159	0.17±0.0038	0.35±0.0051	34.55±0.20

continue...

contuatiion...

Center Pivot 25 - North				Center Pivot 25 - South			
9	0.16±0.0026	0.37±0.0341	32.25±0.58	10	0.16±0.0029	0.34±0.0164	31.85±0.44
41	0.12±0.0010	0.79±0.0112	23.85±0.33	42	0.12±0.0007	0.53±0.0043	23.55±0.29
57	0.12±0.0008	0.89±0.0062	20.65±0.24	58	0.12±0.0009	0.88±0.0043	20.75±0.28
89	0.12±0.0010	0.90±0.0103	24.35±0.43	90	0.12±0.0012	0.90±0.0052	24.55±0.37
105	0.14±0.0021	0.86±0.0154	20.55±0.54	106	0.14±0.0210	0.89±0.0111	21.55±0.32
137	0.14±0.0032	0.40±0.0444	28.45±0.32	138	0.14±0.0039	0.42±0.0233	28.65±0.32
153	0.15±0.0035	0.32±0.0123	31.85±0.27	154	0.14±0.0045	0.40±0.0123	31.95±0.19
169	0.24±0.0067	0.26±0.0094	35.15±1.80	170	0.25±0.0073	0.24±0.0114	37.75±2.03
Center Pivot 26 - North				Center Pivot 26 - South			
8	0.16±0.0030	0.30±0.0133	32.65±0.70	9	0.16±0.0028	0.31±0.0062	33.05±0.69
40	0.12±0.0011	0.40±0.0083	23.95±0.37	41	0.12±0.0008	0.46±0.0041	24.05±0.46
56	0.12±0.0009	0.88±0.0061	20.55±0.48	57	0.12±0.0010	0.88±0.0031	20.15±0.36
88	0.12±0.0013	0.92±0.0041	24.65±0.59	89	0.12±0.0014	0.91±0.0034	24.55±0.39
104	0.14±0.0018	0.86±0.0072	21.55±0.36	105	0.14±0.0020	0.86±0.0074	21.55±0.27
136	0.15±0.0035	0.41±0.0323	29.85±0.23	137	0.14±0.0042	0.48±0.0401	29.55±0.35
152	0.19±0.0028	0.39±0.0134	32.45±0.21	153	0.19±0.0059	0.41±0.0142	32.50±0.28
168	0.25±0.0044	0.24±0.0121	39.65±0.49	169	0.25±0.0071	0.25±0.0172	39.55±0.49

*BS: before sowing.

Between 8 and 10 DAS, which corresponds to the emergence of the first leaf (VE and V1), referring to pivots P25 and P26 North and South, α_s was 0.16, whereas the other center pivots showed values around 0.13 to from 19 DAS. This is because the plant increases leaf density and soil moisture tends to be preserved (Table 3). Sá, Sobrinho, Silva, Ferreira and Moura (2016) pointed out that albedo is very sensitive and can be influenced by the moisture conditions of the soil and plant, humidity, irrigation, land use and the presence of clouds. In areas of irrigated agriculture in the municipality of Jaíba-MG, Brazil, Veloso, Ferreira, Rosa and Silva. (2015) found mean α_s values of the orders of 0.15 and 0.21 in the crop development period and at harvest, respectively. These values are closely linked

to the dynamics of land use in agricultural areas. In contrast, Sá et al. (2016) analyzed the mean daily albedo in the sprouting and emergence phase of the sugarcane crop and observed that the lowest daily mean α_s value was 0.12, considering the high absorption of solar energy, given that the soil had a low biomass density.

The electromagnetic radiation absorbed by plants is known to increase during the period of high vegetative development, due to the peak of photosynthesis. In other words, α_s decreases due to the greater use of incident energy, be it for the processes of photosynthesis or transpiration (Silva, Moura, Giongo, & Silva, 2011). Then, when the plant reduces the photosynthetic rate, α_s increases again.

Throughout the crop development cycle, NDVI showed variations, with a constant increase in the mean. This is explained by the fact that this index grows with the development of the crop, having reached its maximum value around 78 DAS and starting to decline from this point until the senescence of the crop and harvest (Table 3), as the nutrients are displaced for the development of reproductive organs. Subsequently, with maturation, the plant ceases to grow (Alface et al., 2019; Santos et al., 2020). To some extent, NDVI has a positive correlation with biomass gain. However, in the period of high biomass production there is a rapid saturation in the red band. As a consequence, the correlation between NDVI and the leaf area index (LAI) is not so strong in this situation, and so the increase in biomass can no longer be accompanied by the increase in the index values (Jensen, Bryan, Friedman, Henderson, Holz, 1983; Ponzoni & Shimabukuro, 2007).

At the beginning of the crop's phenological cycle, when the soil was exposed, NDVI values were low, ranging from 0.30 to 0.37. Toureiro, Serralheiro, Shahidian and Sousa. (2017) studied the irrigation requirement of maize grown in Mediterranean climatic conditions and found NDVI values close to 0.20 at 10 DAS, in contrast to the 0.34 and 0.37 found in the present study for P25 North and South. This difference in NDVI values is mainly related to the type of soil, amount of soil and straw present in the area. These authors also emphasized on the ability to perform irrigation management based on NDVI.

As also shown in Table 3, the days of higher T_s were also those with the highest RG and air temperature values (Table 2), which coincided with the beginning and end of the crop cycle. This indicates that the plant cover

and the water content in the soil and in the plant have an influence on air temperature. In addition, the vegetative canopy is altered by R_G .

In terms of magnitude, T_s tends to show a behavior inversely proportional to NDVI; i.e., lower T_s values mean higher NDVI. It is worth mentioning that a high T_s value indicates high canopy temperature and, as a consequence, the water content in the leaf is lower than necessary, indicating a possible condition of water stress (Bezerra, Moutra, Silva, Lopes, & Silva, 2014). As stated by Toureiro et al. (2017), when subjected to the condition of water stress in the soil, the maize crop makes use of adaptive survival mechanisms, spending most of the day with the stomata partially closed. As a result, biomass production and grain yield are reduced.

Given that the phenological stage for the maize crop was characterized from the methodology proposed in the FAO-56 report (Allen et al., 1998) and in view of the sensitivity of NDVI to the presence of pigments that participate in photosynthetic and biomass processes in the aerial part (Formaggio & Sanches, 2017; Ribeiro et al., 2017), we estimated the crop coefficient (K_c) from NDVI (Figure 2A). The equation was fitted based on the relationship between NDVI and $K_{c_{FAO}}$ considering the area of the center pivots under study. The high coefficient of determination ($R^2 = 0.789$) denotes that the variance in $K_{c_{FAO}}$ can be explained by NDVI. By analyzing the obtained p-value, it is possible to state that the fit was significant at 0.1% probability. Alface et al. (2019) reported a similar trend, with $R^2 = 0.71$, in an experiment estimating the K_c NDVI of sugarcane in Mozambique. The authors stated that the spectral reflectance was able to provide a fast and accurate estimate of the K_c values.

Figure 2B shows the mean values of Kc_{FAO} for the maize crop and Kc_{NDVI} for all center pivots under study, for each image acquisition date. The mean Kc_{NDVI} values were estimated using the regression equation in Figure 2A. By comparing the behavior of the mean Kc_{FAO} and Kc_{NDVI} values (Figure 2B), we observe that Kc_{FAO} showed a slightly higher trend than Kc_{NDVI} in development stages III and IV. In stages I and II, however, it was lower than the Kc_{NDVI} value estimated over time, with stages I, II, III and IV corresponding to 17%, 28%, 33% and 22%, respectively, of the total cycle (Allen et al.,

1998). This demonstrates that the behavior of Kc_{NDVI} is highly sensitive and directly influenced by aspects of the plant and ground cover. Statistical analysis revealed that it provided good performance, with low errors such as the root mean square error (RMSE = 0.099) and the mean bias error (BIAS = -0.001), $R^2 = 0.85$ and a correlation coefficient (r) of 0.92. It is noteworthy that the mean bias error shows the under- or overestimation of a model; in this respect, there was overestimation in this study.

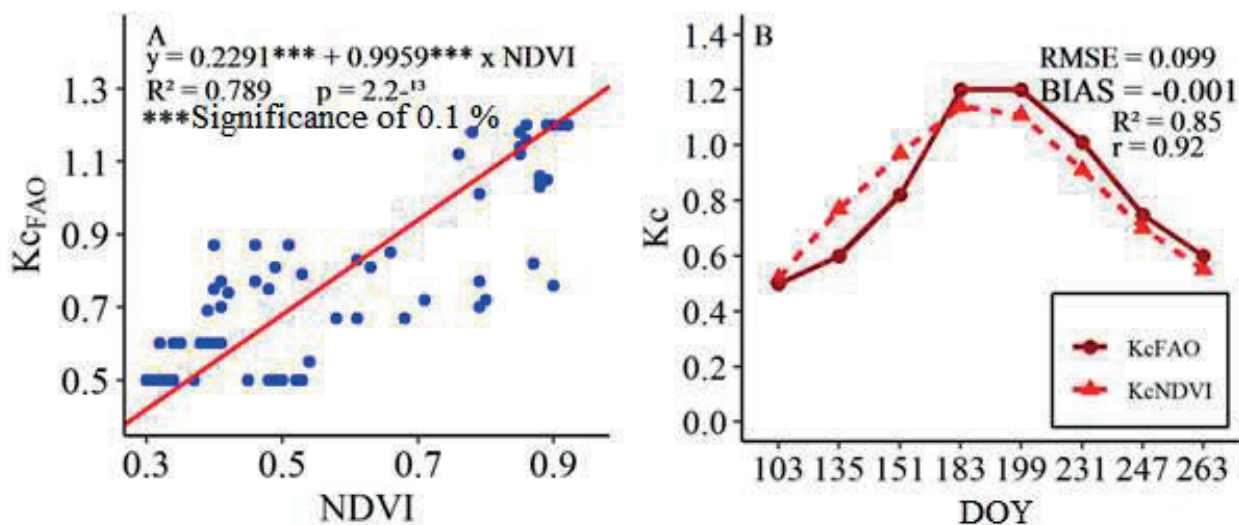


Figure 2. A: Adjusted linear regression between Kc_{FAO} and NDVI values; B: Temporal behavior of the mean Kc_{FAO} and Kc_{NDVI} values of the maize crop. for the different center pivots and orientations. DOY: Day of the year in Julian.

The spatial and temporal values of ET_c acquired by the SAFER algorithm indicate that ET_c is influenced by climatic conditions, soil water content, above-ground biomass and leaf area (Frenck et al., 2018). The daily ET_c values are lower at the beginning of cultivation and increase from the stage of greater

vegetative growth, tasseling and earing, in maize. Thereafter, they decrease when the plant reaches the physiological maturation stage and, subsequently, the physiological components die due to senescence (Figure 3).

Considering the center pivots with different planting dates (Table 1), the ET_c

pixel values ranged from 0.0 to 6.0 mm d⁻¹ throughout the phenological cycle (Figure 4). The highest means were found for DOY 199, corresponding to around 100 DAS, which was because in this physiological stage the soil tends to always remain close to field capacity. In this way, the plants invest in intense photosynthesis, which increases stomatal opening. Additionally, the weather conditions also favored a greater ET_c. On this day, there was little variation in the ET_c data, with the exception of center pivot P25 North, whose values ranged from 3.5 to 6.0 mm d⁻¹. It is worth mentioning that this was the only area planted with cultivar Dekalb 390 Conventional maize, which has a super-early phenological cycle, with an average of 105 days. Another point to be highlighted is the occurrence of the maximum ET_c for P26 (DOY 183, equivalent to 89 DAS).

The second highest mean ET_c value (4.8 mm d⁻¹) occurred at 151 DOY, which corresponds to approximately 45 DAS and represents the period of greatest vegetative development in all center pivots (Figure 4).

Santos et al. (2020) described a similar result in an experiment in which the second-highest ET_c identified in the seed maize crop was close to 5.0 mm d⁻¹, at 46 DAS. It should be noted that, at 231 DOY, center pivots P23 and P24 exhibited low uniformity in their area (Figure 3), with a greater range of data. Another noteworthy factor is the mean, which was less than the median for P23 and P24 East (Figure 4). This was possibly because sowing under these pivots was performed on different dates for different geographic orientations, which had a longer interval relative to the other pivots (P23 North sown on 04/17/2014, P23 South on 04/28/2014, P24 West on 04/16/2014 and P24 East on 04/09/2014). In addition, the low uniformity in each planting orientation can be explained by the fact that the cultivated areas vary in terms of type, texture and physical and water characteristics of the soil under the pivot orientations, as well as plant development. However, the irrigation amount is the same for the entire center pivot area. As a result, certain regions may have been under and/or over irrigated (Santos et al., 2020).

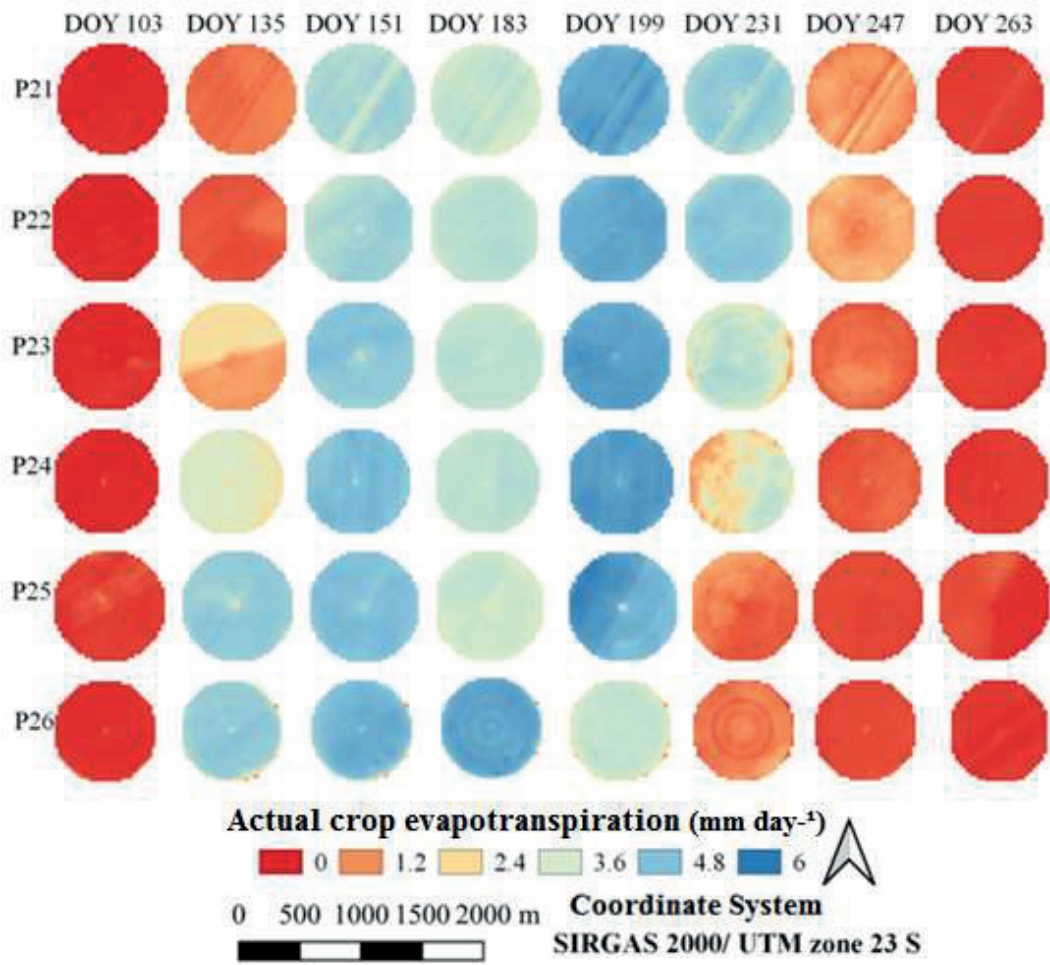


Figure 3. Spatial distribution of actual evapotranspiration (ETc) in the irrigated maize crop.

Figure 5 shows the spatial and temporal distribution of the biomass values accumulated in the maize crop (BIO) in kilograms per hectare, on the days the images

were acquired. The BIO variable represents how much dry matter the plant incorporates per area, per day, in kilograms (Teixeira, Leivas, Andrade, & Hernandez, 2015).

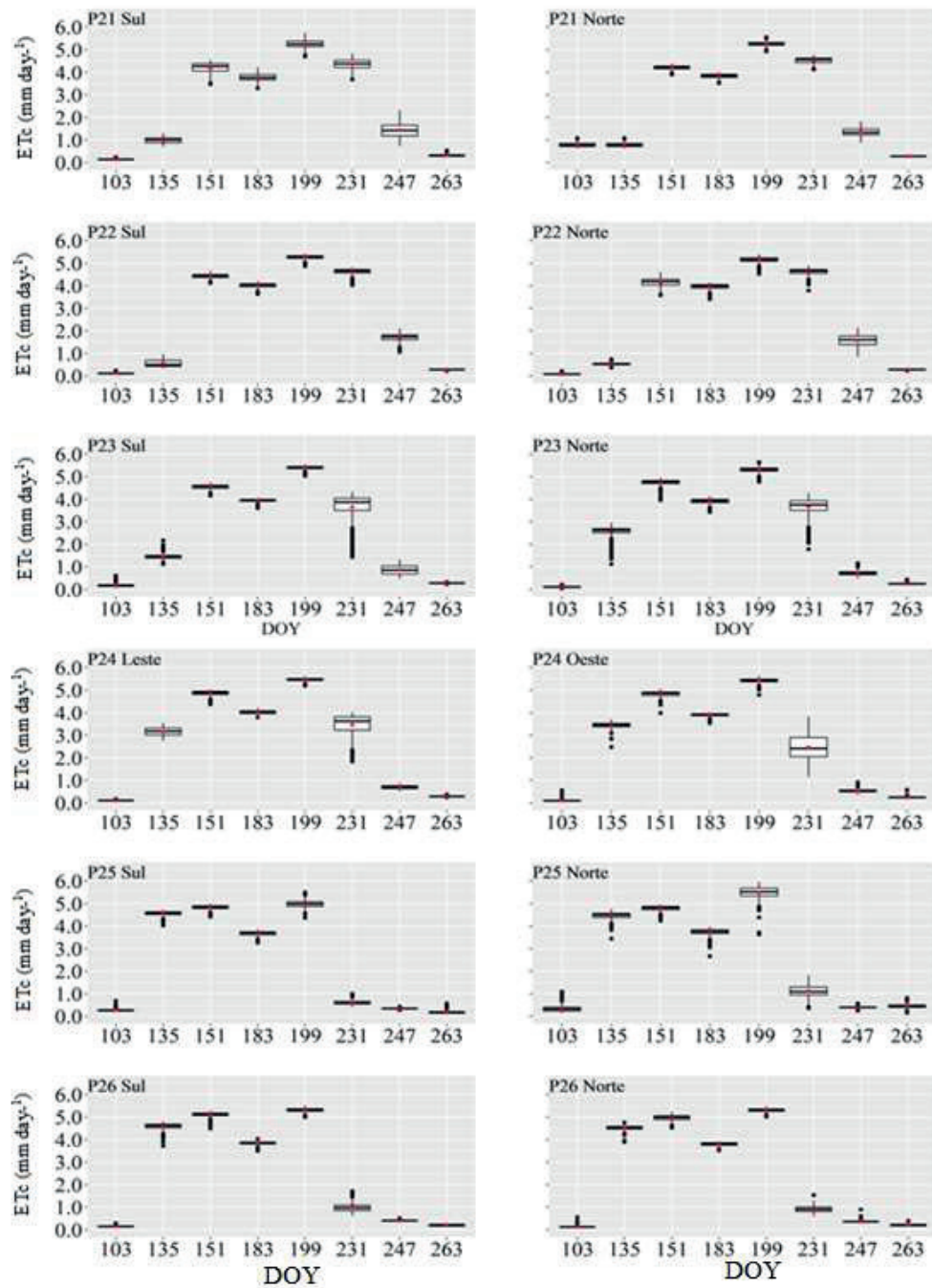


Figure 4. Boxplot of actual evapotranspiration (ET_c) of maize at different stages of development, obtained for the different orientations and center pivots.

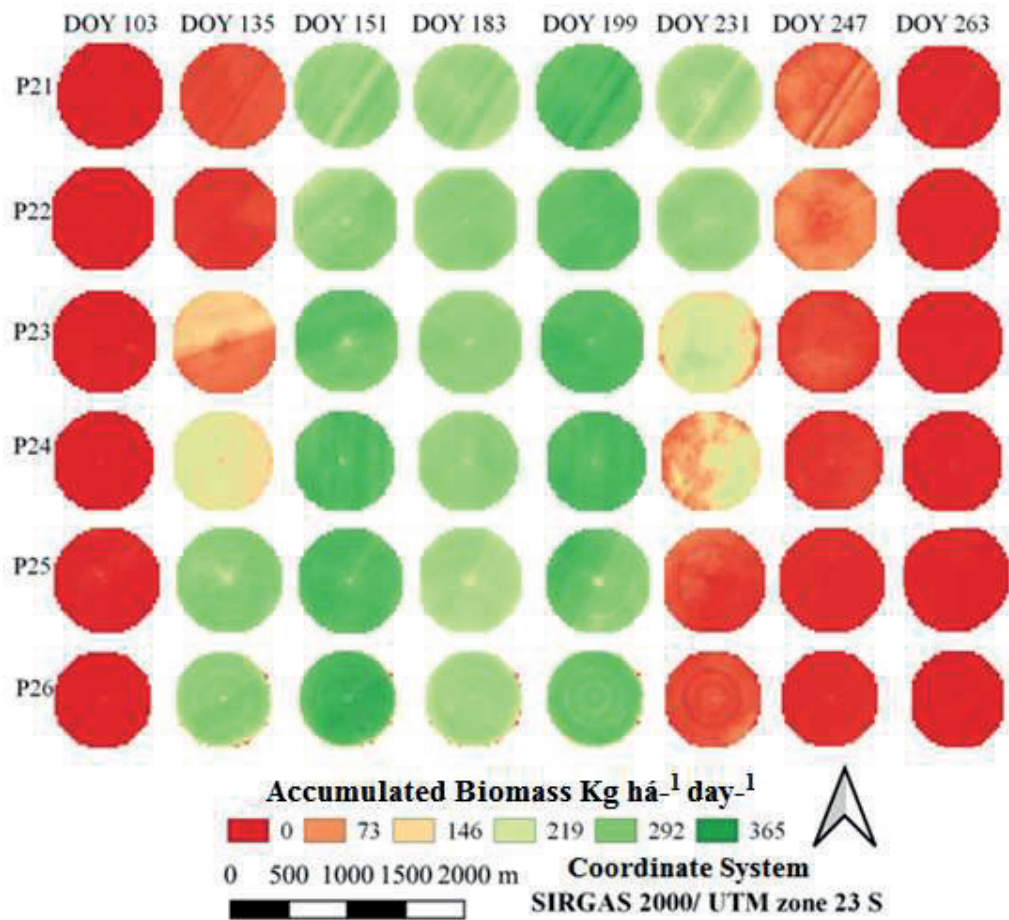


Figure 5. Spatial distribution of accumulated biomass (BIO) in irrigated maize.

The lowest BIO values occurred at 135 DOY, around 20 DAS (Figure 6). On that date, the plants were in the phenological stage characterized by the interval between V2 and V3, when their photosynthetic activity is low due to the reduced leaf area, with mean values close to $45 \text{ kg ha}^{-1} \text{ d}^{-1}$, as seen in center pivots P21 and P22. At 135 DOY, pivot P23 (Figure 6) showed a mean BIO of $50 \text{ kg ha}^{-1} \text{ d}^{-1}$.

Analyzing all the boxplots together, it is clear that the highest BIO values were obtained precisely with the increase in plant development, which is also observed with the increasing NDVI and lower α_s and T_s . This is

because plants are more efficient in converting carbon and light in the photosynthetic system between 135 and 199 DOY, corresponding to 38 to 105 DAS, with values ranging from 220 to $345 \text{ kg ha}^{-1} \text{ d}^{-1}$. After this period, BIO was drastically reduced due to the maturation and later senescence of maize, seen at 150 and 160 DAS, representing 247 and 263 DOY (Santos et al., 2020). The center pivots showed a mean very close to, or equal to the median, which indicates a database with normal behavior, except for P23 oriented South and P24 oriented East. These regions had a mean lower than the median and a greater dispersion of the data.

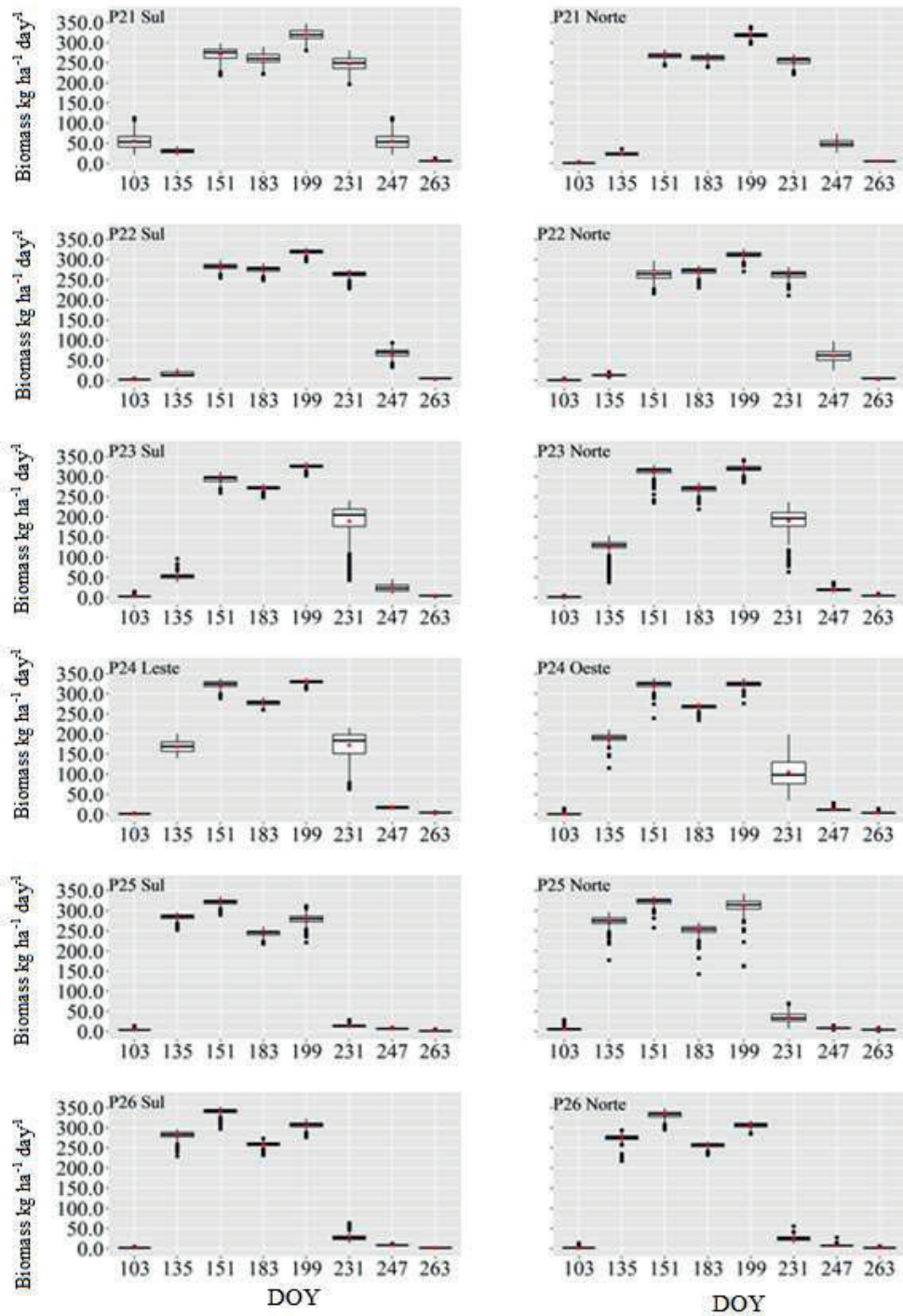


Figure 6. Boxplot of biomass (BIO) of maize at different stages of development. obtained for the different orientations and center pivots.

Because there is a relationship between ET_c and BIO, the DOY with the highest BIO values are equivalent to those with the highest ET_c values (Yuan et al., 2013). In addition to this relationship, BIO is strongly influenced by water availability in the soil, with rainfed crops having higher BIO values during the rainy season and lower under drought conditions. In contrast, irrigated crops achieve higher BIO in the driest periods of the year, as the soils maintain their moisture close to field capacity, from the applied irrigation (Teixeira et al., 2015). However, in irrigated conditions, BIO is also influenced by high air temperature values and low incident solar radiation values (Bhuiyan, Saha, Bandyopadhyay, & Kogan, 2017). In the Nilo Coelho irrigated perimeter, in the semiarid region of Brazil, Teixeira et al. (2015) found that the irrigated maize obtained BIO values twice as high as the species *Alpinia purpurata* in rainfed planting as reported by Wang, Ma, Huang, Veroustraete, Zhang, Song, & Tan. (2012). This leads us to the conclusion that in the study of Teixeira et al. (2015), irrigation was the main factor responsible for the discrepancy in BIO values, besides plant physiology.

Conclusions

The use of remote sensing data from the SAFER algorithm was a relevant tool in the observation of biophysical processes throughout the crop cycle to determine ET_c . With the technique, it was possible to know the spatial-temporal dynamics of ET_c in different physiological phases, indicating the possibility of identifying the irrigation volume to be applied in each location and stage of development of the crop, since the daily actual crop evapotranspiration rates can be dynamic in space and time.

When the plant is at its maximum dry matter increase, NDVI tends to be high. The daily dry matter increases observed in the area under study were similar to those described in studies with the same crop in irrigated areas.

The performance of the methodology used to estimate Kc_{NDVI} provided satisfactory and acceptable results when compared with Kc_{FAO} in maize. As such, it constitutes a great alternative to the tabulated values, with more representative values of Kc in space and with the real conditions throughout the crop cycle.

Acknowledgements

This study was carried out under the support of the Coordination for Improvement of Higher Education Personnel (CAPES) - Brazil, under the Financing Code 001 and by the National Council for Scientific and Technological Development (CNPq).

References

- Alface, A. B., Pereira, S. B., Filgueiras, R., & Cunha, F. F. (2019). Sugarcane spatial-temporal monitoring and crop coefficient estimation through NDVI. *Revista Brasileira de Engenharia Agrícola e Ambiental*, 23(5), 330-335. doi: 10.1590/1807-1929/agriambi
- Allen, R. G., Pereira, L. S., Raes, D., & Smith, M. (1998). *Crop evapotranspiration - guidelines for computing crop water requirements - FAO Irrigation and drainage paper 56* (9th ed.). Rome: Food and Agriculture Organization of the United Nations.

- Althoff, D., Santos, R. A., Bazame, H. C., Cunha, F. F., & Filgueiras, R. (2019). Improvement of hargreaves-samani reference evapotranspiration estimates with local calibration. *Water*, *11*(11), 22-72. doi: 10.3390/w11112272
- Bastiaanssen, W. G. M., & Ali, S. (2003). A new crop yield forecasting model based on satellite measurements applied across the Indus Basin, Pakistan. *Agriculture, Ecosystems e Environment*, *94*(3), 321-340. doi: 10.1016/S0167-8809(02)00034-8
- Bernardo, S., Mantovani, E. C., Silva, D. D., & Soares, A. A. (2019). *Manual de irrigação* (9a ed.). Viçosa, MG: Imprensa Universitária da UFV.
- Bezerra, J. M., Moutra, G. B. A., Silva, B. B., Lopes, P. M. O., & Silva, E. F. F. (2014). Parâmetros biofísicos obtidos por sensoriamento remoto em região semiárida do estado do Rio Grande do Norte, Brasil. *Revista Brasileira de Engenharia Agrícola e Ambiental*, *18*(1), 73-84.
- Bhuiyan, C., Saha, A. K., Bandyopadhyay, N., & Kogan, F. N. (2017). Analyzing the impact of thermal stress on vegetation health and agricultural drought - a case study from Gujarat, India. *Journal GIScience & Remote Sensing*, *54*(5), 1943-7226. doi: 10.1080/15481603.2017.1309737
- Congedo, L. (2016). *Semi-automatic classification plugin documentation: release 5.0.1.1*. Roma: Sapienza University of Rome.
- Formaggio, A. R., & Sanches, I. A. (2017). *Sensoriamento remoto na agricultura*. São Paulo: Oficina de Textos.
- Frenck, G., Leitinger, G., Obojes, N., Hofmann, M., Newesely, C., Deutschmann, M.,... Tasser, E. (2018). Community-specific hydraulic conductance potential of soil water decomposed for two Alpine grasslands by small-scale lysimetry. *Biogeosciences*, *15*(1), 1065-1078. doi: 10.5194/bg-15-1065-2018
- Higuchi, N., Santos, J., Ribeiro, R. J., Minette, L., & Biot, Y. (1998) Biomassa da parte aérea da vegetação de floresta tropical úmida de terra-firme da Amazônia Brasileira. *Acta Amazônica*, *28*(1), 153-165. doi: 10.1590/1809-43921998282166
- Jensen, J. R., Bryan, M. L., Friedman, S. Z., Henderson, F. M., Holz, R. K., Lindgren, D.,... Wray, J. R. (1983). Urban/suburban land use analysis. In J. E. Estes (Ed.), *Manual of remote sensing* (vol. 2, pp. 1571-1666, 2nd ed.). Falls Church, VA: American Society of Photogrammetry.
- Martins, C. L., Busato, C., Silva, S. F., Rodrigues, W. N., & Reis, E. F. (2013). Avaliação do desempenho de sistemas de irrigação no sul do Estado do Espírito Santo. *Revista Agro@ambiente*, *7*(2), 236-241. doi: 10.18227/1982-8470ragro.v7i2.1069
- Monteith, J. L. (1972). Solar radiation and productivity in tropical ecosystems. *Journal of Applied Ecology* *9*(3), 747-766. doi: 10.2307/2401901
- Pandey, P. K., Dabral, P. P., & Pandey, V. (2016). Evaluation of reference evapotranspiration methods for the Northeastern region of India. *International Soil and Water Conservation Research*, *4*(1), 56-67. doi: 10.1016/j.iswcr.2016.02.003

- Ponzoni, F. J., & Shimabukuro, Y. E. (2007). *Sensoriamento remoto no estudo da vegetação*. São José dos Campos: Ed. Parêntese.
- QGIS Development Team (2015). *QGIS Geographic information system (3.16)*. Retrieved from <http://www.qgis.org/>
- R Core Team (2016). *R: A language and environment for statistical computing*. Vienna, Austria: R Foundation for Statistical Computing. Retrieved from <https://www.R-project.org/>
- Ribeiro, R. B., Filgueiras, R., Ramos, M. C. A., Almeida, L. T., Generoso, T. N., & Monteiro, L. I. B. (2017). Variação espacial-temporal da condição da vegetação na agricultura irrigada por meio de imagens sentinela. *Revista Brasileira de Agricultura Irrigada*, 11(1), 1884-1893. doi: 10.7127/rbai.v11n600648
- Rissini, A. L. L., Kawakami, J., Genú, A. M. (2015). Índice de vegetação por diferença normalizada e produtividade de cultivares de trigo submetidas a doses de nitrogênio. *Revista Brasileira de Ciência do Solo*, 39(6), 1703-1713. doi: 10.1590/01000683rbcs20140686
- Rouse, J. W., Haas, R. H., Schell, J. A., & Deering, D. W. (1974). Monitoring vegetation systems in the great plains with ERTS. *Proceedings of the Earth Resources Technology Satellite-1, Symposium*, Greenbelt, 3.
- Sá, P. C. C., Sobrinho, J. S., Silva, S. T. A., Ferreira, R. C., & Moura, M. S. B. (2016). Estimativa do saldo de radiação em cultivo irrigado de cana-de-açúcar utilizando dados de sensoriamento remoto orbital. *Revista Brasileira de Geografia Física*, 9(7), 2164-2178. doi: 10.5935/1984-2295.20160153
- Santos, R. A., Venancio, L. P., Filgueiras, R., & Cunha, F. F. (2020). Remote sensing as a tool to determine biophysical parameters of irrigated seed corn crop. *Semina: Ciências Agrárias*, 41(2), 435-446. doi: 10.5433/1679-0359.2020v41n2p435
- Silva, A. P. N., Moura, G. B. A., Giongo, P. R., & Silva, B. B. (2011). Albedo de superfície estimado a partir de imagens Landsat 5 - TM no Semiárido Brasileiro. *Revista de Geografia*, 27(1), 154-168.
- Silva, B. B., Braga, A. C., Braga, C. C., Oliveira, L. M. M., Montenegro, S. M. G., & Barbosa, B., Jr. (2016). Procedures for calculation of the albedo with OLI-Landsat 8 images: application to the Brazilian semi-arid. *Revista Brasileira de Engenharia Agrícola e Ambiental*, 20(1), 3-8. doi: 10.1590/1807-1929
- Teixeira, A. H. C. (2010). Determining regional actual evapotranspiration of irrigated and natural vegetation in the São Francisco riverbasin (Brazil) using remote sensing Penman-Monteith equation. *Remote Sensing*, 2(5), 1287-1319. doi: 10.3390/rs0251287
- Teixeira, A. H. C., & Leivas, J. F. (2017). Determinação da produtividade da água com imagens Landsat 8 na região Semiárida do Brasil. *Revista Conexões Ciência e Tecnologia*, 11(1), 22-34. doi: 10.21439/conexoes.v11i1.1064
- Teixeira, A. H. C., Leivas, J. F., Andrade, R. G., & Hernandez, F. B. T. (2015). Water productivity assessments with Landsat 8 images in the Nilo Coelho irrigation scheme. *Revista Irriga*, 1(2), 1-10. doi: 10.15809/irriga.2015v1n2p01

- Teixeira, A. H. C., Scherer-Warren, M., Hernandez, F. B., Andrade, R. G., & Leivas, J. F. (2013). Large-scale water productivity assessments with modis images in a changing semi-arid environment: a brazilian case study. *Remote Sensing, Multidisciplinary Digital Publishing Institute*, 5(11), 5783-5804. doi: 10.3390/rs5115783
- Toureiro, C., Serralheiro, R., Shahidian, S., & Sousa, A. (2017). Irrigation management with remote sensing: Evaluating irrigation requirement for maize under Mediterranean climate condition. *Agricultural Water Management*, 184(1), 211-220. doi: 10.1016/j.agwat.2016.02.010
- United States Geological Survey (2015). *Landsat Project Description*. Recuperado de http://landsat.usgs.gov/about_project_descriptions.php.
- Vanhellemont, Q., & Ruddick, K. (2014). Turbid wakes associated with of shore wind turbines observed with landsat 8. *Remote Sensing of Environment*, 145(1), 105-115. doi: 10.1016/j.rse.2014.01.009
- Veloso, G. A., Ferreira, M. E., Rosa, R., & Silva, B. B. (2015). Determinação do albedo de superfície em áreas irrigadas do projeto Jaíba (Minas Gerais) mediante imagens Landsat 5 - TM. *Revista R. Ra'eGa*, 35(1), 126-146. doi: 10.5380/raega.v35i0.39757
- Wang, X., Ma, M., Huang, G., Veroustraete, F., Zhang, Z., Song, Y., & Tan, J. (2012). Vegetation primary production estimation at maize and alpine meadow over the Heihe River Basin, China. *International Journal of Applied Earth Observation Geoinformation*, 17(1), 94-101. doi: 10.1016/j.agrformet.2018.01.005
- Yuan, M., Zhang, L., Gou, F., Su, Z., Spiertz, J. H. J., & Van. W. W. (2013). Assessment of crop growth and water productivity for five C3 species in semi-arid Inner Mongolia. *Agricultural Water Management*, 122(5), 28-38. doi: 10.1016/j.agwat.2013.02.006

